Saturation Spectra of the Two-Plasmon Decay Instability

D. F. DuBois,[1] D. A. Russell,[2] and Harvey A. Rose[1]
[1]*Los Alamos National Laboratory, MS-B213, Los Alamos, New Mexico 87545*
[2]*Lodestar Research Corporation, 2400 Central Avenue P-5, Boulder, Colorado 80301*
(Received 6 October 1994)

A nonlinear, reduced description of the saturated steady-state turbulence resulting from the two-plasmon decay instability is shown to lead to Langmuir wave and $\frac{3}{2}\omega_0$ radiation spectra which are in semiquantitative agreement with recent experimental observations of Meyer *et al.* [Phys. Rev. Lett. **71**, 2915 (1993)]. Secondary Langmuir wave decay of the primary unstable waves is shown to be an important process for moderate laser intensities while strong turbulence effects are observed for higher intensities.

PACS numbers: 52.35.Nx, 52.35.Ra, 52.40.Nk

The two-plasmon decay (TPD) instability has been the subject of many theoretical [1] and experimental [2] studies beginning with the work of Goldman in 1966. This Letter describes preliminary results of an attempt to model the global nonlinear development of the TPD on relatively long space and time scales. Recent experiments of Meyer and Zhu [3] employed Thomson scattering diagnostics to measure the **k**-space distribution of Langmuir (plasma) waves excited by a CO_2 laser in a long scale-length ($\sim$2 mm) nitrogen plasma via the TPD instability. In this and in a previous experiment by Meyer, Zhu, and Curzon [4] the angular distribution and power spectra of the emitted $\frac{3}{2}\omega_0$ diagnostic radiation from the laser-induced Langmuir turbulence were also measured. In this Letter we compare the predictions, for these spectra, of our reduced nonlinear model of TPD to these observations.

It is a well-known problem that the primary unstable Langmuir waves cannot couple locally to the $\frac{3}{2}\omega_0$ light. Propagation of these waves in the density gradient has been invoked, but it was shown by Meyer in 1992 [1] that under typical conditions these waves will be collisionally damped before matching can occur. A new result reported here is that there is efficient *local* coupling with secondary Langmuir decay waves and that this coupling leads to the observed angular distribution and *power spectrum* of the $\frac{3}{2}\omega_0$ light.

TPD occurs at electron densities n_0 near one-quarter of the laser critical density n_C and may play an important role in the laser-plasma interaction regimes relevant to inertial confinement fusion. It provides an anomalous absorption mechanism by which the laser energy is converted into hot electrons. Greatly enhanced superthermal levels of low-frequency density fluctuations, which are mainly ion acoustic waves, have been predicted by Langdon, Lasinski, and Kruer and by Kartunnen [1] and in our studies. The long-wavelength, ponderomotively driven, density fluctuations may be manifest in density profile modification near $n_0 \sim \frac{1}{4}n_C$ [1,2].

The reduced nonlinear model for our studies, derived in Sagdeev *et al.* [1] and in Ref. [5], employs an equation for the complex envelope $\mathbf{E}(\mathbf{x},t)$ of the Langmuir fluctuations, where the physical Langmuir electric field is expressed as $\frac{1}{2}\mathbf{E}(\mathbf{x},t)\exp(-i\omega_p t)$ + c.c. and where $|\partial_t \mathbf{E}|/|\mathbf{E}| \ll \omega_p \equiv (4\pi e^2 n_0/m_e)^{1/2}$:

$$\nabla\cdot\left[2i\omega_p(\partial_t + \nu_e\circ) + 3v_e^2\nabla^2 - \left(\frac{4\pi e^2}{m_e}\right)n\right]\mathbf{E}(x,y,t) = \frac{e}{4m_e}\nabla\cdot[\nabla(\mathbf{E}_0\cdot\mathbf{E}^*) - \mathbf{E}_0\nabla\cdot\mathbf{E}^*]. \quad (1)$$

Here the pump or laser field of frequency ω_0 has only an x component of the form $\mathcal{E}_0\exp(i[k_0 y - \Omega_0 t])$, corresponding to a plane wave traveling in the y direction, where $\mathbf{E}_0$ is the envelope of this field with respect to the frequency $2\omega_p$, and therefore $\Omega_0 = \omega_0 - 2\omega_p$. The wave number is $k_0 = (3/4)^{1/2}\omega_0/c$ plus terms of order Ω_0/ω_0. $v_e^2 = T_e/m_e$ is the electron thermal velocity squared and n_0 is the background or reference electron density. The equation satisfied by the low-frequency density fluctuation, $n(x,y,t)$, about this reference density, which is driven by the ponderomotive pressure of the high-frequency waves, is

$$[\partial_t^2 + 2\nu_i\circ\partial_t - c_s^2\nabla^2]n = (16\pi m_i)^{-1}\nabla^2|\mathbf{E}|^2, \quad (2)$$

where $c_s^2 = (ZT_e + 3T_i)/m_i$ is the ion acoustic wave speed squared.

Equations (1) and (2) have the form of driven and damped Zakharov equations and have the usual validity conditions [5,6]. In this Letter we will present the results of two-dimensional (2D) numerical simulations of solutions of these equations. As in previous studies [6], the operator ν_e, which is local in **k** space, is the sum of collisional and Landau damping of Langmuir waves (LW's). The Landau damping models the coupling to hot electrons, and ν_i is the corresponding Landau damping of ion acoustic waves (IAW's).

To study the $\frac{3}{2}\omega_0$ radiation we compute the *transverse* current envelope with respect to $3\omega_p \simeq \frac{3}{2}\omega_0$,

$$\mathbf{J}_{3/2}(x,y,t) = \frac{e}{4\pi i\omega_0 m_e}(\mathbf{E}_0\nabla\cdot\mathbf{E})_{\text{trans}}, \quad (3)$$

which is the leading term [5] for this emission involving the beating of the laser with the TPD-induced LW's. This

radiation is emitted in all directions at the wave number $k_{3/2} = (8/3)^{1/2}k_0$ (plus terms of order Ω_0/ω_0). Thus the Poynting flux is proportional to $|\mathbf{J}_{3/2}(\mathbf{k}_{3/2}, t)|^2$ where only the *direction* of $\mathbf{k}_{3/2}$ is varied. We see immediately from Eq. (3) that no $\frac{3}{2}\omega_0$ radiation is emitted in the direction of $\mathbf{E}_0$. This is consistent with the observations of Meyer, Zhu, and Curzon [3,4].

We have carried out dozens of 2D, homogeneous, periodic simulations [6] with at least 128 × 128 Fourier modes and typically 10^3 electron Debye lengths in each direction. The parameters were originally chosen to be representative of a large class of experiments and are close to those appropriate for Meyer, Zhu, and Curzon [3,4]. The parameter choices which matter for this problem are $k_0\lambda_D \sim \sqrt{3}\,v_e/c = 0.05$ and $\nu_e(0)/\omega_{p_0} \simeq \nu_{ei}/\omega_0 \simeq 2 \times 10^{-4}$, which are appropriate for a nitrogen plasma with a mean charge state $\bar{Z} \simeq 4$ and temperature of ~400 eV. The ion temperature was not measured and we have taken $\bar{Z}T_e/T_i \simeq 10$ corresponding to a moderately weak ion acoustic damping $\nu_i(k)/kc_S \simeq 0.05$.

In Fig. 1 we show examples of time-averaged (denoted by brackets $\langle\cdots\rangle$) modal energy spectra of Langmuir wave fluctuations $k^2\langle|\mathbf{E}(\mathbf{k})|^2\rangle$ (proportional to the high-frequency electron density spectra) for two laser strengths at two different values of n_0/n_C in the quasistationary saturated state. The locations of the linearly most unstable modes in $k^2\langle|\mathbf{E}(\mathbf{k})|^2\rangle$ are marked with four smaller (solid) circles. In the initial linear evolution these modes grow at the predicted linear growth rates, but upon saturation the spectrum becomes much richer. In addition to crescents of neighboring linearly (but somewhat less) unstable modes, new islands (marked with diamonds) appear corresponding to the Langmuir wave decay (i.e., LW → LW′ + IAW) of the primary unstable modes. Baldis and Walsh [2] have observed a shift of the saturated LW spectrum toward lower-k values with increasing but relatively lower laser intensities which may be consistent with secondary Langmuir wave decay. The corresponding decay ion acoustic waves are also seen in the $\langle|n(\mathbf{k})|^2\rangle$ spectra [5]. These secondary decay features are most prominent at lower values of n_0/n_C and for weaker laser drives E_0. For increasing n_0/n_C or E_0 these features broaden and a near-isotropic underlying spectrum, broadening toward higher k, grows which we attribute to Langmuir caviton excitation. At higher laser intensities, Baldis and Walsh [2] report a broadening of the Langmuir wave spectrum toward higher-k values with increasing intensity, again consistent with our observations in this regime. At the highest densities, approaching $n_0/n_C = 0.25$, the decay features are not distinct, and caviton activity dominates even for drives near threshold ($E_0/E_T \sim 2$). A useful measure of caviton activity is the (time- and space-averaged) correlator $-\langle n|\mathbf{E}|^2\rangle/\langle|n|^2\rangle^{1/2}\langle|\mathbf{E}|^2\rangle$, which is 0.5 or greater in the cases of strong caviton activity referred to above [5]. Positive values indicate a correlation between localized Langmuir wave packets $|\mathbf{E}|^2$ and the density depletions (or wells) that entrain them. In all the cases considered here the saturation levels of LW's are well below wave breaking or electron trapping levels.

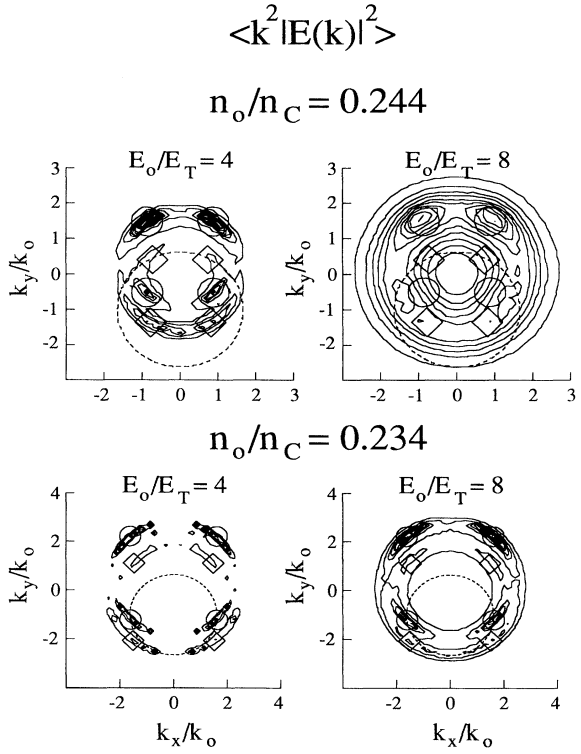

FIG. 1. Contours of the spectral energy distribution $k^2\langle|\mathbf{E}(\mathbf{k})|^2\rangle$ in (k_x, k_y) space for two values of n_0/n_C and two laser strengths E_0/E_T. The laser $\mathbf{E}_0$ is polarized along the x axis with $\mathbf{k}_0$ along the y axis. The laser strength is measured in terms of the damping threshold value E_T for TPD: $\frac{1}{4}(eE_T/m\omega_0)k_0 \equiv \nu_e(k = 0)$. Smaller solid circles superimposed on the E-field spectra are centered on the linearly most unstable wave vectors, while diamonds are centered on their decay product. Wave vectors on the larger dashed circle can contribute to $\frac{3}{2}\omega_0$ radiation. In the figures we plot dimensionless quantities: electric fields in units of $(64\pi\eta n_0 T_e/3M)^{1/2}$, lengths in units of $3/2M^{1/2}\lambda_{De}$, time in units of $3/2M\omega_p^{-1}$, and densities in units of $\frac{4}{3}n_0M^{-1}$ where $M \equiv m_i/\eta m_e$ and $\eta \equiv c_s^2/(T_e/m_i)$.

Using the electric field fluctuations calculated in the quasisaturated state we can compute the time-averaged $\frac{3}{2}\omega_0$ current using Eq. (3) and so produce the $\frac{3}{2}\omega_0$ radiation patterns shown in Fig. 2 for the same parameters as in Fig. 1. For a given emission angle θ, between $\mathbf{k}_{3/2}$ and $\mathbf{k}_0$, the $\mathbf{k}$-matching condition $\mathbf{k}_{3/2} = \mathbf{k}_0 + \mathbf{k}_L$ requires that the Langmuir wave number $k_L(\theta)$ satisfies $k_L^2(\theta)/k_0^2 = \frac{11}{3} - 2(8/3)^{1/2}\cos(\theta)$. These k_L values lie on the dashed "radiation" circles shown in Fig. 1. We see from the intersections of the radiation circles with the intense regions of $k^2\langle|\mathbf{E}(\mathbf{k})|^2\rangle$ that the forward-scattered lobes at $\theta \simeq 30° \pm 10°$ seen at higher n_0/n_C ($n_0/n_C = 0.244$ in Fig. 2) are caused by the Thomson up-conversion off the forward-going (relative to $\mathbf{k}_0$) secondary LW's (e.g., the upper pair of diamonds in Fig. 1 for $n_0/n_C = 0.244$ and $E_0/E_T = 4$)

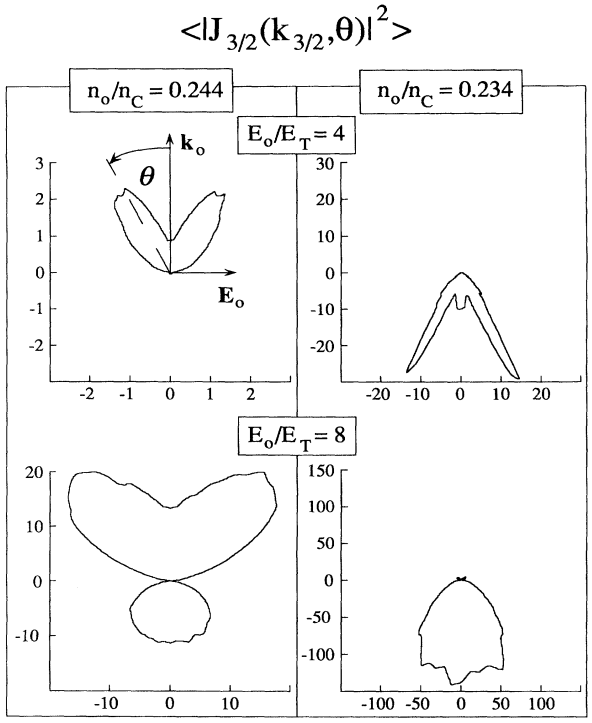

FIG. 2. Polar plots of the $\frac{3}{2}\omega_0$ radiation intensity as a function of angle for the same cases as in Fig. 1. The horizontal (x) axis is $-\sin(\theta)$ times the intensity at θ and the vertical (y) axis is $\cos(\theta)$ times the intensity.

resulting from the decay of the backward-going primary unstable waves. Likewise, the backward-scattered lobes at $\theta \simeq 156° \pm 5°$ seen at lower n_0/n_C ($n_0/n_C = 0.234$ in Fig. 2) result from the scattering of the incident radiation off the backward-going secondary LW's (e.g., the lower pair of diamonds in Fig. 1 for $n_0/n_C = 0.234$ and $E_0/E_T = 4$) resulting from the decay of the forward-going primary LW's.

The power spectra $\langle|\mathbf{J}_{3/2}(\mathbf{k}_{3/2},\omega)|^2\rangle$ of the $\frac{3}{2}\omega_0$ radiation were obtained from time series of $\mathbf{J}_{3/2}(\mathbf{k}_{3/2},t)$ lasting about 2 ns. We find that the forward lobes at higher density ($n_0/n_C = 0.244$) are redshifted spectral peaks but become very broad for $E_0/E_T = 8$ while the backward lobes at lower density ($n_0/n_C = 0.234$) are blueshifted and narrower. The peak emission frequency that results from the up-scattering (anti-Stokes) of the laser from a free LW is simply $\omega - \frac{3}{2}\omega_0 = -\frac{1}{2}\Omega_0 + \frac{3}{2}\omega_p k_L^2(\theta)\lambda_D^2$ and this accounts approximately for the shifts of the strong emission lobes calculated in the simulations. This formula implies that the shifts relative to $\frac{3}{2}\omega_0$ depend on density ($\Omega_0/\omega_p = \sqrt{n_C/n_0} - 2$) and emission angle θ. Higher n_0/n_C always favors blueshifted light; but, with increasing n_0/n_C, backscattered light becomes blueshifted at a lower density than does forward-scattered light. This is contrary to some predictions based on the coupling of $\frac{3}{2}\omega_0$ radiation to the primary unstable modes in a density gradient (e.g., see Seka *et al.*, 1985 [2]), but it is probably consistent with the observations of Young *et al.* [2]. The broadening of the spectra with increasing E_0 and/or n_0/n_C is due to trapped (or bound) caviton fields which have significant power at frequencies *less* than the local plasma frequency, which translates into $\omega - \frac{3}{2}\omega_0 < -\frac{1}{2}\Omega_0$ for the emitted radiation. Big redshifts from forward-scattered $\frac{3}{2}\omega_0$ radiation for n_0/n_C approaching 0.25 appear to be evidence for collapse.

To make contact with observations in long scale-length plasmas with $n_0 \leq \frac{1}{4}n_C$ it is necessary to take into account the weak density inhomogeneity which we take here to be in the $\mathbf{k}_0$ (i.e., the y) direction only. If the scale length $L \gg \ell_C$, where the correlation length is defined by

$$\ell_C = \frac{\partial/\partial k_y \langle\langle|\mathbf{E}(k_x,k_y,\{n_0\})|^2\rangle\rangle}{\langle\langle|\mathbf{E}(k_x,k_y,\{n_0\})|^2\rangle\rangle}, \tag{4}$$

it can be shown that the spatially averaged spectrum, such as $\langle\langle|\mathbf{E}(\mathbf{k})|^2\rangle\rangle$, can be represented as an incoherent superposition of spectra:

$$\begin{aligned}\langle\langle|\mathbf{E}(\mathbf{k})|^2\rangle\rangle &\simeq L^{-1}\int_0^L dy\,\langle|\mathbf{E}(\mathbf{k},\{n_0(y)\})|^2\rangle \\ &= L^{-1}\int_{n_0\,\min}^{n_0\,\max} dn_0 (dn_0/dy)^{-1}\langle|\mathbf{E}(\mathbf{k},\{n_0(y)\})|^2\rangle .\end{aligned} \tag{5}$$

This method of spatial averaging applies to all spectra.

To make contact with the long scale-length experiments of Meyer, Zhu, and Curzon [4], the integral in Eq. (5) was performed using a discrete set of simulation spectra at nine density points in the range $0.2 < n_0/n_C < 0.25$. The density profile $n_0(y)$ is not known in detail, and we have varied it to obtain an "eyeball" best fit to the experimental data for the modal energy spectrum $\langle\langle|\mathbf{E}(k_x,k_y)|^2\rangle\rangle$, the angular distribution of $\frac{3}{2}\omega_0$ radiation $\langle\langle|\mathbf{J}_{3/2}(k_{3/2},\theta)|^2\rangle\rangle$, and the power spectrum $\langle\langle|\mathbf{J}_{3/2}(k_{3/2},\theta,\omega)|^2\rangle\rangle$. The details of the latter two quantities appeared to be most sensitive to the profile. A monotonically decreasing profile led to the best fit shown in the inset to Fig. 3 which also shows the contours of the resulting $\langle\langle|\mathbf{E}(k_x,k_y)|^2\rangle\rangle$ for $E_0/E_T = 4$ and 8. These spectra can be compared to the one in Fig. 5 of Meyer and Zhu [3]. The theory and experiment agree in a semiquantitative way; the wave energy is concentrated in the same regions of $\mathbf{k}$ space. However, the shapes of the intensity contours differ. The simulation contours are based on a uniform grid of points in $\mathbf{k}$ space, whereas the experimental data were taken along fifteen discrete arcs in $\mathbf{k}$ space [3]. We believe, and J. Meyer agrees (private communication), that the experimental data analysis imposes the geometry of the arcs on the contours. The density-averaged angular distribution of $\frac{3}{2}\omega_0$ radiation shown in Fig. 4 is in excellent agreement for $E_0/E_T = 4$ with the observations of Meyer, Zhu, and Curzon [3,4], showing a forward peak at $\theta \sim 36° \pm 5°$ and a backward peak at $\theta \sim 150° \pm 5°$. For $E_0/E_T = 8$ the calculations predict more $\frac{3}{2}\omega_0$ radiation at $\theta = 180°$

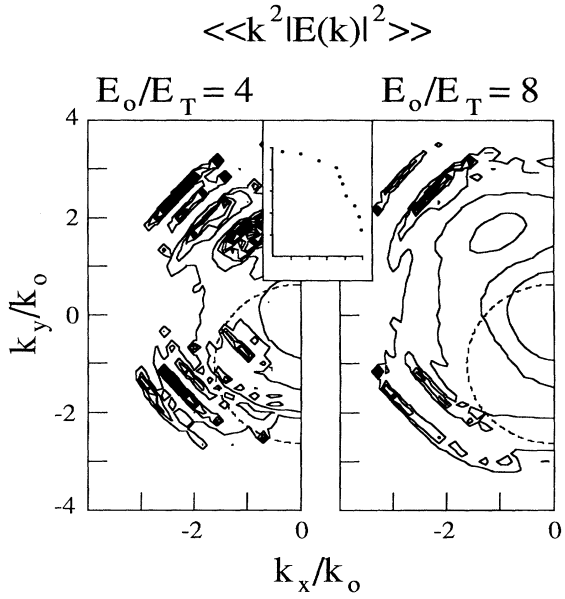

FIG. 3. $\langle\langle k^2|\mathbf{E}(k_x,k_y)|^2\rangle\rangle$, density-averaged energy spectra for the two cases $E_0/E_T = 4$ and 8 and for the density profile shown in the inset. Inset: $n_0(y)/n_C$ on [0.2,0.25] vs y/L on [0,1]; L is arbitrary.

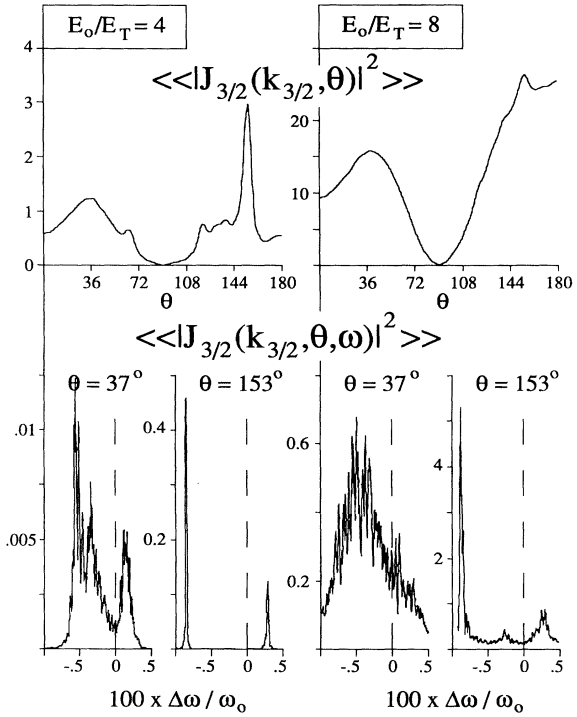

FIG. 4. Density-averaged angular distribution of $\frac{3}{2}\omega_0$ radiation and power spectra at the angles of maximum forward ($\theta = 37°$) and of maximum backward ($\theta = 153°$) emission for the two cases of Fig. 3. A dashed line indicates zero shift. The sharpness of the spectral peaks, e.g., at $\theta = 153°$ and $E_0/E_T = 4$, is an artifact of the sparse density sampling.

than observed. The power spectra of the $\frac{3}{2}\omega_0$ radiation in the directions of these maxima are also in qualitative agreement with the observations of Meyer, Zhu, and Curzon [4], showing very broad, probably collapse-dominated, spectra (especially for $E_0/E_T = 8$) in the forward lobe, and in the backward lobe a distinct redshifted peak on a broad, partly blueshifted pedestal.

The best agreement with the observations appears to be obtained for laser strengths in the range $4 < E_0/E_T < 8$. Translated into intensities, these are roughly an order of magnitude less than the putative experimental intensities of several times 10^{13} W/cm^2. For higher intensities we predict broader spectra and more $\frac{3}{2}\omega_0$ emission at $\theta = 180°$ than observed. The TPD activity, however, was observed [3] for about 350 ps during the rising portion of a 2 ns (FWHM) pulse when the intensity was below average. The convective loss of TPD plasmons due to the finite transverse extent ($\sim$140 μm) of the laser beam also will raise the effective threshold above the homogeneous-plasma damping threshold of our simulations. Further experimental and theoretical studies are needed to see if these effects can account for the difference in intensities.

We have also studied the consequences of the high level of ion acoustic fluctuations in the saturated state of TPD on Brillouin scattering of ω_0 light and emission of $\frac{1}{2}\omega_0$ light [5]. A reasonable future challenge for experiment is to measure by Thomson scattering the **k**-space distribution of low-frequency fluctuations to compare with theory [5].

We wish to acknowledge fruitful conversations with Jochen Meyer and Hector Baldis. This research was supported by the United States Department of Energy.

[1] M. V. Goldman, Ann. Phys. (N.Y.) **38**, 117 (1966); C. S. Liu and M. N. Rosenbluth, Phys. Fluids **19**, 967 (1976); A. R. Simon, R. W. Short, E. A. Williams, and T. Devandre, *ibid.* **26**, 3107 (1983); A. B. Langdon, B. F. Lasinski, and W. L. Kruer, Phys. Rev. Lett. **43**, 133 (1979); S. J. Kartunnen, Plasma Phys. **22**, 151 (1980); A. M. Rubenchik, Sov. Phys. JETP **41**, 498 (1975); D. F. DuBois and B. Bezzerides, Phys. Rev. Lett. **36**, 729 (1976); R. Z. Sagdeev, G. I. Solov'ev, V. D. Shapiro, V. I. Schevchenko, and I. V. Yusupov, Sov. Phys. JETP **55**, 74 (1982); H. H. Chen and C. S. Liu, Phys. Rev. Lett. **39**, 881 (1977); J. Meyer, Phys. Fluids B **4**, 2934 (1992).

[2] H. A. Baldis and C. J. Walsh, Phys. Rev. Lett. **47**, 1658 (1981); D. M. Villeneuve, H. A. Baldis, and C. J. Walsh, Phys. Fluids **28**, 1454 (1985); K. A. Tanaka *et al.*, Phys. Fluids **28**, 2910 (1985); W. Seka *et al.*, *ibid.* **28**, 2570 (1985); P. E. Young *et al.*, Phys. Rev. Lett. **61**, 2766 (1988); W. Seka *et al.*, Phys. Fluids B **4**, 2232 (1992).

[3] J. Meyer and Y. Zhu, Phys. Rev. Lett. **71**, 2915 (1993).

[4] J. Meyer, Y. Zhu, and F. L. Curzon, Phys. Fluids B **1**, 650 (1989).

[5] D. F. DuBois, D. A. Russell, and H. A. Rose (to be published).

[6] D. F. DuBois, A. Hanssen, H. A. Rose, and D. Russell, Phys. Fluids B **5**, 2616 (1993); J. Geophys. Res. **98**, 17 543 (1993).